Geochemistry Geophysics Geosystems G3
AN ELECTRONIC JOURNAL OF THE EARTH SCIENCES
Published by AGU and the Geochemical Society

*Characterization*
Volume 8, Number 4
3 April 2007
Q04I16, doi:10.1029/2006GC001444
ISSN: 1525-2027

Click Here for Full Article

# Chemical composition of sediments subducting at the Izu-Bonin trench

**Terry Plank**
*Department of Earth Sciences, Boston University, 685 Commonwealth Avenue, Boston, Massachusetts 02215, USA (tplank@bu.edu)*

**Katherine A. Kelley**
*Department of Earth Sciences, Boston University, 685 Commonwealth Avenue, Boston, Massachusetts 02215, USA*
*Now at Graduate School of Oceanography, University of Rhode Island, Narragansett, Rhode Island 02882, USA*

**Richard W. Murray**
*Department of Earth Sciences, Boston University, 685 Commonwealth Avenue, Boston, Massachusetts 02215, USA*

**Lacie Quintin Stern**
*Department of Earth Sciences, Boston University, 685 Commonwealth Avenue, Boston, Massachusetts 02215, USA*
*Now at Sumner G. Whittier School, Everett, Massachusetts 02149, USA*

[1] In this characterization brief, report here comprehensive major and trace element analyses of over 45 sediment samples from Ocean Drilling Program Site 1149, located seaward of the Izu-Bonin trench. The combination of these core analyses with a complete set of geochemical logging data enables us to calculate the bulk composition of the sedimentary column subducting at the Izu trench with high accuracy (uncertainties $\leq$13%). Izu sediment has lower concentrations than global subducting sediment for most elements, due to $\sim$50% dilution by biogenic material ($\sim$45% opal and $\sim$10% carbonate), but is relatively enriched in Ba, Pb, and rare earth elements (REE), except Ce, due to nonterrigenous inputs. Sediments subducting into the Izu and Mariana trenches differ compositionally due to ocean island–sourced volcaniclastics in Marianas sediments, enriching them in Nb, Ta, Ti, and LREE, and continentally derived eolian material in Izu sediments, enriching them in Cs, Rb, Th, and U. These differences predict along-strike variations in sediment input that should be manifested in the composition of volcanic output from the Honshu-Izu-Bonin-Mariana arc systems. Such variations are observed as an increase in Th/La in both sediments and arc volcanics from the Marianas in the south to Honshu in the north.

**Components:** 14,019 words, 7 figures, 4 tables.

**Keywords:** subduction; ODP 185; geochemistry; Mariana; Izu.

**Index Terms:** 1030 Geochemistry: Geochemical cycles (0330); 1031 Geochemistry: Subduction zone processes (3060, 3613, 8170, 8413); 1051 Geochemistry: Sedimentary geochemistry.

**Received** 11 August 2006; **Revised** 21 November 2006; **Accepted** 15 January 2007; **Published** 3 April 2007.

Plank, T., K. A. Kelley, R. W. Murray, and L. Q. Stern (2007), Chemical composition of sediments subducting at the Izu-Bonin trench, *Geochem. Geophys. Geosyst.*, *8*, Q04I16, doi:10.1029/2006GC001444.

Copyright 2007 by the American Geophysical Union

**Theme:** Oceanic Inputs to the Subduction Factory
**Guest Editors:** J. Ludden and T. Plank

## 1. Introduction

[2] The Izu-Bonin-Mariana (IBM) convergent margin (Figure 1) is currently a focus of community effort in problems related to recycling within the "Subduction Factory" [*Stern et al.*, 2003; *Tatsumi*, 2005]. Here, a variety of outputs effuse through the upper plate at different distances from the trench, including (1) serpentine muds, fluids and blueschists in the IBM fore-arcs, (2) classic island arc volcanism of the Marianas and Izu arcs, and (3) back-arc volcanism in the Mariana Trough and Sumisu Rift. For this reason, the IBM system has been chosen as a MARGINS focus site, to study the recycling of material from the oceanic input on the down-going plate to the variety of outputs on the overriding plate. A prerequisite in such a study is accurate measurement of input fluxes into the trench. Thus Leg 185 of the Ocean Drilling Program (ODP) was dedicated to drilling altered oceanic crust and sediment entering the IBM system [*Plank et al.*, 2000]. One site, ODP 1149, was drilled specifically to provide the first complete section of the sedimentary column entering the Izu trench (Figure 1). The purpose of this brief is to use Site 1149 to provide an accurate estimate of the chemical composition of sediments subducting at the Izu trench. This study is a companion to *Kelley et al.* [2003], which uses Leg 185 materials to provide a bulk chemical composition for the altered oceanic crust entering the IBM system.

## 2. Background Geology

[3] ODP Site 1149 lies in the Nadezhda Basin, approximately 100 km east of the Izu-Bonin trench (31°20.5′N, 143°21.1′E), on a slight bathymetric high, where the Pacific plate is flexed upward before it enters the subduction zone (Figure 1). The age of basement is early Cretaceous (Valanginian, Chron M12R, 134 Ma), based on magnetic anomaly lineations, and radiolarian assemblages and carbon isotope stratigraphy in the basal sediments [*Bartolini*, 2003; *Plank et al.*, 2000].

[4] The following summary is extracted from the Initial Reports for Site 1149 [*Plank et al.*, 2000] (see also Figure 2). Site 1149 begins with normal mid ocean ridge volcanism, formed at medium spreading rates (51 km/Ma) in the early Cretaceous southern ocean (~5°S). Aside from fracture-filling sediment (Unit V), the first major sedimentary unit above basement consists of interbedded radiolarian chert and radiolarian nannofossil chalk/marl (Unit IV), reflecting the high primary productivity of subequatorial paleolatitudes. This unit also records waning hydrothermal inputs as the site moved away from the mid-ocean ridge (see V. Chavagnac et al. (Investigating "hydrothermal" inputs to the Izu-Bonin subduction factory: Leg 185 Site 1149B, manuscript in preparation, 2007) for a more detailed discussion). As the site moved north, calcareous sediments no longer accumulated, and 127–105 Ma sediments [*Bartolini*, 2003] consist of alternating clay and chert (Unit III). Dark brown pelagic clay (Unit II) accumulated as the site moved out of the equatorial biogenic sedimentation belt and into the central gyre of the Pacific. Ichthyolith abundance is high in the lower portion of this unit, due in part to the low sedimentation rate. As the site approached the Izu-Bonin trench, the Kuroshio current, and the westerly wind belt, volcanic ash-bearing diatom/radiolarian clay accumulated from 6.5 Ma up to the present (Unit I). Most of the history of the site (~100 Ma) is recorded in the slowly depositing (<1 m/Ma), poorly dated, metal-rich Unit II clays, with more rapid sedimentation occurring in lower biogenic units (~5 m/Ma in Unit III, and ~20 m/Ma in Unit IV) and the upper eolian unit (increasing upward from 7–34 m/Ma in Unit I). Thus Site 1149 recovered a classic oceanic sedimentary section that records the site's journey from an equatorial biogenic-dominated regime (Units III–V), to a slow sedimentation-rate pelagic clay regime (Unit II), to an eolian-dominated pelagic clay regime (Unit I).

## 3. Sampling and Analytical Methods

### 3.1. Major and Trace Element Analyses of Core Samples

[5] Because the primary goal of this study is to provide a bulk geochemical estimate of the sedimentary column subducting at the Izu-Bonin trench, samples were taken of representative lithologies from Site 1149 sediments, at evenly spaced intervals downcore. Samples were freeze-dried, and then powdered in an alumina ball-mill or

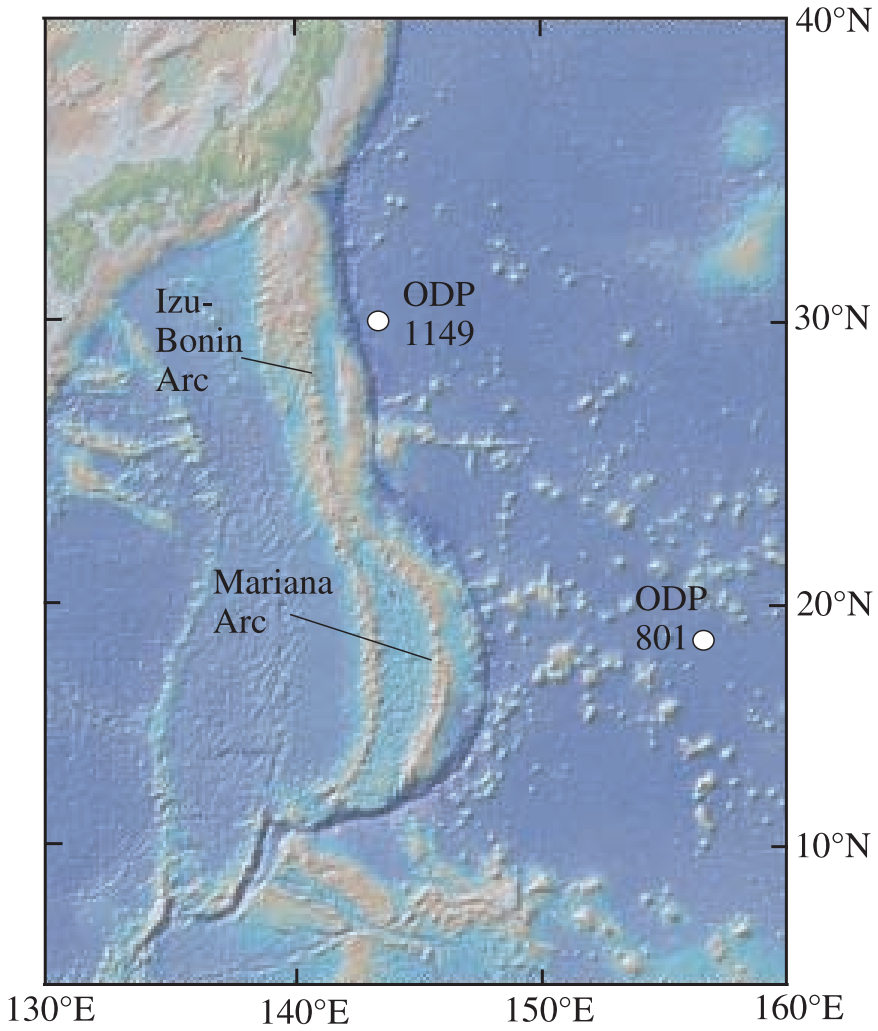


**Figure 1.** Location of ODP Site 1149, reference site for sediment subducting at the Izu-Bonin trench. Basemap made with GeoMapApp.

alumina shatterbox to provide 10–40 grams of powder. A total of 95 samples were analyzed for major elements, Sr and Ba by inductively coupled plasma emission spectrometry (ICP-ES, Table 1), with a sub-set of 45 samples also analyzed for trace elements by inductively coupled plasma mass spectrometry (ICP-MS, Table 2). Methods of chemical preparation and instrumental analysis generally follow procedures outlined by *Kelley et al.* [2003]; further details are given in the footnotes to Tables 1 and 2. Within-run precision was assessed through multiple replicate analyses of the natural samples, and is quantified to be 1–3% relative for Ca, Fe, Mg, Mn, Sr, Ti; 3–5% for Al, P, Si, Ba, Na; 8–10% for K, and ≤2% relative for all elements measured by ICP-MS. External precision is 3–4% on average, based on 5–6 different aliquots of standard reference materials prepared and analyzed with the Site 1149 sediments (Table 2). There is no evidence for zircon (and therefore under-recovery of Zr) in these deep-sea sediments, based on the similarity in the Hf isotopic composition for open-beaker versus Parr bomb digestions (within 0.1 epsilon unit for 1149 sediments; C. Chauvel, personal communication, 2006), and based on tests run with similar pelagic sediments (e.g., IOBC in Table 2). An effort has been made to provide aliquots of Site 1149 sediment powders for various geochemical studies [*Sadofsky and Bebout*, 2004; *Hauff et al.*, 2003; *Valentine et al.*, 2002; *Rouxel et al.*, 2002, 2003a, 2003b; *Chauvel et al.*, 2006], and interested investigators are encouraged to contact the first author.

## 3.2. Geochemical Logging Data

[6] Geochemical logging data are typically used qualitatively, to refine stratigraphic interpretations,

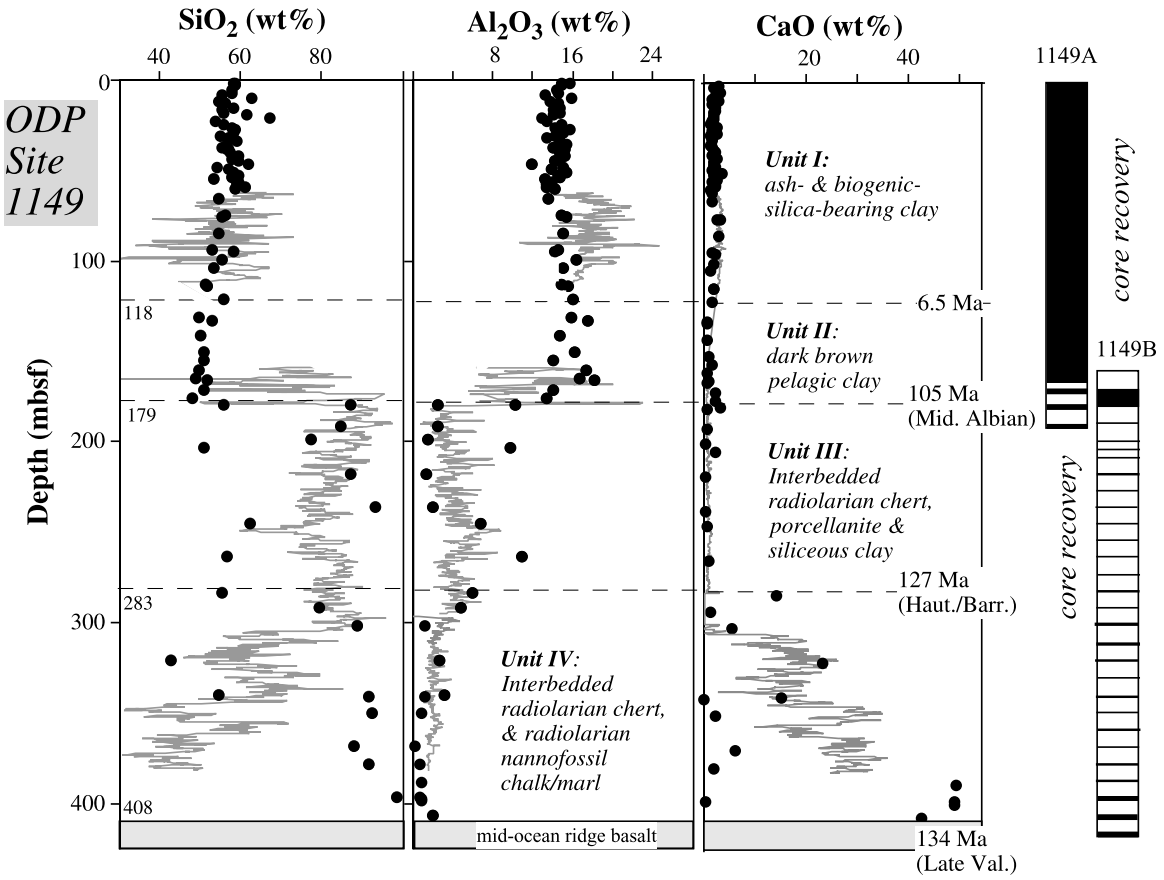


**Figure 2.** Summary of the sedimentary column subducting at the Izu trench, from ODP Site 1149. Core recovery, unit thicknesses, and age boundaries from *Plank et al.* [2000] and *Bartolini* [2003]. Comparison of geochemical logging tool (GLT) data (gray line) and ICP-ES major element bulk analyses of sediment core samples (solid circles). GLT data corrected as described in text and Table 3. Note good agreement between logging data and core analyses. The average of the log-derived $SiO_2$ in Unit I agrees within ~1% relative of the core average (Table 4). Agreement in core-log $SiO_2$ is good for chert-rich compositions in Unit III but not for clay-rich compositions (50–60% $SiO_2$ in core samples). This is due to the sampling of clay beds that are thinner than the 1-meter footprint of the GLT measurements. A similar issue occurs in Unit IV, where thin chert beds (>88 wt% $SiO_2$) are not sampled by the GLT. Thus mismatches in the data are largely an issue of sampling thin beds that are smoothed in the logging signal, and not an error in the calibration of the logging data, which seem accurate. Note four carbonate-rich core analyses from 390–408 mbsf with $SiO_2$ < 12 wt% do not plot at this scale. $Al_2O_3$ shows some of the same issues as $SiO_2$, but the logging data are less accurate, being systematically offset to higher values.

but with some care, accurate chemical information can also be obtained [*Plank and Ludden*, 1992]. During Leg 185, the geochemical logging tool string (GLT) was run in Hole 1149B, irradiating the formation and measuring Al, Si, Fe, Ca, Ti, S, Gd and K in situ [*Plank et al.*, 2000]. A continuous section was collected from 63 mbsf (above which was pipe) to within ~20 m of the basement (385 mbsf), with the exception of a 50 m section largely within Unit II, where the hole was constricted (Figure 2). Thus the GLT sampled ~65% of the sedimentary section, and almost 90% of Units III and IV where recovery was very low (<10%). The natural gamma activity of Hole 1149B was also measured in each logging run (prior to irradiation), providing in situ concentrations of K, Th and U (Figure 3). We use the natural gamma data from the most complete run, the hostile environment natural gamma sonde on the triple combo tool, which recorded emissions from 63–400 mbsf, or 82% of the sedimentary section. Although no longer routine with ODP, the use of the GLT was particularly valuable during Leg 185 because of the poor recovery in the chert-rich units (<10%), and because of the geochemical goals of the leg. In order to make a detailed comparison between core analyses and logging data, we correct the GLT data for assumptions made about the concentrations of elements not measured, and we correct the natural gamma K-Th-U data for water/porosity of the

**Table 1 (Representative Sample).** Major Element Analyses of ODP 1149 Sediments[a] [The full Table 1 is available in the HTML version of this article at http://www.g-cubed.org.]

| Hole | | Core | Sec | Interval, cm | Type[b] | Depth, mbsf | Unit | $SiO_2$, wt% | $TiO_2$, wt% | $Al_2O_3$, wt% | $Fe_2O_3$, wt% | MnO, wt% | MgO, wt% | CaO, wt% | $Na_2O$, wt% | $K_2O$, wt% |
|---|---|---|---|---|---|---|---|---|---|---|---|---|---|---|---|---|
| 1149 | A | 1H | 2 | 68–70 | XRF | 2.18 | I | 58.35 | 0.595 | 15.80 | 5.86 | 0.174 | 2.44 | 2.43 | 4.35 | 2.60 |
| 1149 | A | 1H | 2 | 140–150 | IWS | 2.90 | I | 58.88 | 0.602 | 14.83 | 5.19 | 0.204 | 1.93 | 1.99 | 4.11 | 3.32 |
| 1149 | A | 2H | 1 | 140–150 | IWS | 5.60 | I | 57.79 | 0.659 | 14.42 | 6.91 | 0.143 | 2.66 | 3.35 | 3.29 | 1.98 |
| 1149 | A | 2H | 2 | 140–150 | IWS | 7.10 | I | 57.73 | 0.681 | 14.54 | 7.33 | 0.162 | 2.64 | 2.14 | 3.73 | 2.37 |
| 1149 | A | 2H | 3 | 140–150 | IWS | 8.60 | I | 55.28 | 0.611 | 13.31 | 5.83 | 0.731 | 2.61 | 1.76 | 3.32 | 2.42 |
| 1149 | A | 2H | 4 | 140–150 | IWS | 10.10 | I | 62.67 | 0.739 | 15.86 | 7.18 | 0.127 | 2.81 | 2.80 | 3.56 | 2.46 |
| 1149 | A | 2H | 5 | 140–150 | **IWS | 11.60 | I | 54.54 | 0.619 | 13.71 | 6.32 | 0.334 | 2.70 | 1.62 | 2.75 | 2.76 |
| 1149 | A | 2H | 6 | 140–150 | IWS | 13.10 | I | 56.11 | 0.662 | 14.62 | 6.24 | 0.120 | 2.26 | 2.42 | 3.19 | 2.05 |
| 1149 | A | 3H | 1 | 140–150 | IWS | 15.10 | I | 58.38 | 0.657 | 14.77 | 6.10 | 0.315 | 2.55 | 2.24 | 2.92 | 2.32 |
| 1149 | A | 3H | 2 | 140–150 | IWS | 16.60 | I | 55.43 | 0.563 | 14.04 | 5.95 | 0.121 | 2.33 | 1.92 | 3.16 | 2.34 |
| 1149 | A | 3H | 3 | 140–150 | **IWS | 18.10 | I | 55.86 | 0.664 | 14.66 | 6.41 | 0.110 | 2.55 | 2.01 | 2.95 | 2.41 |
| 1149 | A | 3H | 4 | 140–150 | IWS | 19.60 | I | 61.66 | 0.570 | 14.16 | 5.23 | 0.090 | 2.06 | 1.93 | 3.43 | 2.71 |
| 1149 | A | 3H | 5 | 140–150 | IWS | 21.10 | I | 67.36 | 0.262 | 12.92 | 1.73 | 0.143 | 0.67 | 1.66 | 4.00 | 3.53 |
| 1149 | A | 3H | 6 | 140–150 | IWS | 22.60 | I | 53.88 | 0.619 | 13.49 | 5.90 | 0.174 | 2.56 | 1.24 | 2.95 | 2.56 |
| 1149 | A | 4H | 1 | 140–150 | IWS | 24.60 | I | 55.66 | 0.662 | 14.83 | 6.98 | 0.120 | 2.65 | 2.67 | 3.24 | 2.30 |
| 1149 | A | 4H | 2 | 140–150 | **IWS | 26.10 | I | 57.72 | 0.637 | 14.28 | 7.08 | 0.121 | 2.71 | 1.46 | 2.74 | 2.53 |
| 1149 | A | 4H | 3 | 140–150 | IWS | 27.60 | I | 58.76 | 0.689 | 15.80 | 6.47 | 0.122 | 2.79 | 2.50 | 3.33 | 2.59 |
| 1149 | A | 4H | 4 | 140–150 | IWS | 29.10 | I | 58.20 | 0.647 | 15.07 | 6.11 | 0.110 | 2.60 | 1.26 | 2.96 | 2.80 |
| 1149 | A | 4H | 5 | 140–150 | IWS | 30.60 | I | 54.86 | 0.608 | 14.23 | 5.19 | 0.365 | 2.36 | 1.51 | 2.94 | 2.78 |
| 1149 | A | 4H | 6 | 140–150 | IWS | 32.10 | I | 57.08 | 0.490 | 13.38 | 4.70 | 0.097 | 1.87 | 1.61 | 3.45 | 2.45 |
| 1149 | A | 5H | 1 | 140–150 | IWS | 34.10 | I | 58.93 | 0.636 | 14.75 | 5.64 | 0.117 | 2.34 | 1.44 | 3.07 | 2.97 |
| 1149 | A | 5H | 2 | 140–150 | IWS | 35.60 | I | 56.74 | 0.686 | 15.41 | 6.85 | 0.128 | 2.71 | 1.69 | 2.70 | 2.77 |
| 1149 | A | 5H | 3 | 140–150 | IWS | 37.10 | I | 55.48 | 0.629 | 14.14 | 5.64 | 0.096 | 2.37 | 1.89 | 3.18 | 2.42 |
| 1149 | A | 5H | 4 | 69–73 | XRF | 37.89 | I | 56.78 | 0.655 | 15.25 | 6.50 | 0.120 | 2.58 | 2.21 | 4.13 | 2.53 |
| 1149 | A | 5H | 4 | 140–150 | IWS | 38.60 | I | 56.87 | 0.687 | 15.01 | 6.34 | 0.105 | 2.55 | 1.78 | 2.92 | 2.43 |
| 1149 | A | 5H | 5 | 140–150 | **IWS | 40.10 | I | 57.51 | 0.625 | 14.77 | 5.81 | 0.100 | 2.45 | 1.55 | 2.74 | 2.71 |
| 1149 | A | 5H | 6 | 140–150 | IWS | 41.60 | I | 59.40 | 0.679 | 15.21 | 6.04 | 0.134 | 2.08 | 2.57 | 3.27 | 2.34 |
| 1149 | A | 6H | 1 | 140–150 | IWS | 43.60 | I | 57.71 | 0.602 | 14.76 | 5.91 | 0.177 | 2.37 | 1.98 | 2.95 | 2.55 |
| 1149 | A | 6H | 2 | 140–150 | IWS | 45.10 | I | 59.32 | 0.598 | 14.32 | 6.54 | 0.209 | 2.47 | 1.78 | 3.37 | 2.58 |
| 1149 | A | 6H | 3 | 140–150 | IWS | 46.60 | I | 61.79 | 0.670 | 11.99 | 6.03 | 0.539 | 2.29 | 2.24 | 3.60 | 2.21 |

[a] ICP-ES analyses performed at Boston University, generally following procedures outlined by *Kelley et al.* [2003]. Sample powders were ignited at 900°C for 1 hour to measure loss on ignition (LOI) and then mixed with lithium metaborate and fused at 1050°C for 15 minutes. Molten beads were dissolved in 5% nitric acid, filtered, and diluted by mass to a final solution of 1:4000 in 2% $HNO_3$. High carbonate samples were not ignited prior to fusion, in order to minimize alkali loss [*Plank and Ludden*, 1992]. Separate aliquots of these samples were then ignited to determine LOI. A procedural blank as well as the following standard reference materials were prepared in the same manner as the unknowns: K1919 (Kilauea basalt), QLO-1 (USGS quartz latite), SDC-1 (USGS mica schist), BCSS-1 (marine mud), SCo-1 (USGS Cody shale), JA-1 (GSJ andesite), AGV-1 (USGS andesite), W-2 (USGS diabase). Data were reduced by blank subtraction, external drift correction, and standard calibration, using values of *Kelley et al.* [2003]. Calibrations were strongly linear ($R2 > 0.999$). Concentrations are reported relative to weight of freeze-dried powders. Some data reported overspecified for calculation purposes.

[b] The double asterisks (**) indicate a common sample shared for major elements, trace elements, and isotopes. IWS, interstitial water squeeze cake samples; complementary pore waters reported by *Plank et al.* [2000]. XRF, powdered on ship; shipboard XRF analysis reported by *Plank et al.* [2000]. XRF samples analyzed by ICP-ES here for comparison; agreement between two techniques is 1–3% for Si, Al, Fe, Ca, and Sr; 4–6% for Mn, Mg, Na, K, and Ba; and 10–15% for Ti, P, and LOI.

**Table 2 (Representative Sample).** Trace Element Composition of ODP 1149 Sediments[a] [The full Table 1 is available in the HTML version of this article at http://www.g-cubed.org.]

| Hole | | 1149A | 1149A | 1149A | 1149A | 1149A | 1149A | 1149A | 1149A | 1149A | 1149A | 1149A | 1149A | 1149A | 1149A | 1149A |
|---|---|---|---|---|---|---|---|---|---|---|---|---|---|---|---|---|
| Core-sec | -cm | 1H1-140 | 2H5-140 | 3H3-140 | 4H2-140 | 5H5-140 | 6H5-140 | 7H4-140 | 8H3-140 | 9H3-140 | 10H3-140 | 11H3-140 | 12H3-140 | 13H4-15 | 14H2-140 | 15H3-106 |
| Lithol. Descr. | | ash & diat clay | rad & ash clay | clay | clay | clay | clay | ash & silty clay | clay | ash & diat clay | ash & diat clay | diatom clay | ash-rich clay | clay | clay | mottled clay |
| Depth | mbsf | 1.4 | 11.6 | 18.1 | 26.1 | 40.1 | 49.6 | 57.6 | 65.6 | 75.1 | 84.6 | 94.1 | 103.6 | 113.35 | 121.1 | 131.76 |
| Interval | m | 6.5 | 8.35 | 7.25 | 11 | 11.75 | 8.75 | 8 | 8.75 | 9.5 | 9.5 | 9.5 | 9.625 | 9.525 | 8.43 | 10.25 |
| Unit | Iso. | I | I | I | I | I | I | I | I | I | I | I | I | I | IIA | IIA |
| Be | 9 | 1.58 | 1.87 | 1.88 | 1.95 | 1.82 | 1.14 | 1.37 | 1.75 | 1.66 | 1.56 | 2.24 | 2.04 | 1.80 | 2.14 | 2.13 |
| Sc | 45 | 19.7 | 17.0 | 17.9 | 17.9 | 16.4 | 21.9 | 18.5 | 16.1 | 20.8 | 20.1 | 17.5 | 17.9 | 22.7 | 24.3 | 20.7 |
| $TiO_2$ | 49 | 0.602 | 0.564 | 0.634 | 0.627 | 0.608 | 0.622 | 0.605 | 0.516 | 0.689 | 0.628 | 0.589 | 0.642 | 0.68 | 0.69 | 0.635 |
| V | 51 | 158 | 118 | 127 | 123 | 130 | 135 | 92.5 | 100 | 137 | 132 | 94 | 117 | 152 | 194 | 136 |
| Cr | 52 | 40.6 | 55.4 | 56.3 | 61.6 | 59.8 | 34.6 | 32.7 | 46.1 | 49.3 | 35.7 | 54.1 | 60.4 | 51.4 | 52.2 | 47.5 |
| Co | 59 | 16.4 | 18.2 | 19.6 | 15.8 | 19.4 | 21.2 | 15.0 | 20.3 | 21.4 | 32.8 | 25.8 | 24.4 | 36.3 | 47.8 | 67.1 |
| Ni | 60 | 32.7 | 59.8 | 47.0 | 54.0 | 52.1 | 31.4 | 31.1 | 45.8 | 38.4 | 43.8 | 52.8 | 54.9 | 53.4 | 66.6 | 87.4 |
| Cu | 65 | 62.5 | 75.1 | 93.1 | 84.0 | 81.9 | 77.3 | 47.0 | 69.8 | 202 | 131 | 175 | 148 | 143 | 156 | 180 |
| Zn | 66 | 89.7 | 104 | 97.7 | 95.9 | 97.1 | 91.2 | 96.2 | 87.8 | 93.6 | 88.5 | 95.0 | 97.1 | 100 | 106 | 108 |
| Ga | 69 | 16.8 | 16.2 | 17.5 | 17.8 | 18.0 | 16.0 | 16.1 | 16.7 | 18.8 | 16.4 | 18.2 | 19.2 | 18.3 | 18.6 | 20.4 |
| Rb | 85 | 77.4 | 101 | 94.1 | 98.8 | 110 | 63.7 | 62.0 | 86.6 | 91.4 | 71.9 | 102 | 117 | 97.4 | 97.1 | 107 |
| Sr | 88 | 143 | 131 | 154 | 130 | 139 | 149 | 149 | 142 | 151 | 143 | 131 | 117 | 117 | 113 | 112 |
| Y | 89 | 24.9 | 20.0 | 22.9 | 23.1 | 27.5 | 24.8 | 30.6 | 24.9 | 29.0 | 27.1 | 34.2 | 29.6 | 27.9 | 26.2 | 35.8 |
| Zr | 90 | 84.7 | 75.8 | 86.7 | 90.4 | 97.1 | 80.2 | 92.1 | 85.8 | 89.8 | 94.6 | 100 | 99.4 | 95.5 | 90.4 | 96.4 |
| Nb | 93 | 6.24 | 9.20 | 9.48 | 8.82 | 9.99 | 5.64 | 5.43 | 8.36 | 7.79 | 6.31 | 10.7 | 10.2 | 9.64 | 8.52 | 8.66 |
| Cs | 133 | 5.85 | 7.05 | 7.22 | 7.43 | 8.71 | 4.72 | 4.91 | 6.35 | 7.68 | 5.84 | 8.22 | 9.88 | 7.80 | 8.53 | 8.67 |

[a] ICP-MS analyses carried out at Boston University, following procedures of *Kelley et al.* [2003], although variants on these techniques were applied to accommodate various sedimentary lithologies. Silicate-rich samples were dried at 100°C and then were weighed into screw-top Teflon vials, dissolved overnight in HF and HNO3, and dried down at 90°C. Dried samples were re-wetted with DI water and hydrogen peroxide to digest organic matter. Solutions were then acidified with HNO3, transferred to 250 mL HDPE bottles, diluted with DI water to 4000x the original dry powder weight, and sonicated for 30 minutes. Carbonate-rich samples were first attacked with $HNO_3$ only and then were centrifuged and the supernatant drawn off. This step dissolves the carbonate component without allowing calcium fluoride to precipitate during HF attack. The solid residue was then dissolved following the above procedure for silicate-rich samples. A procedural blank as well as standard reference materials (SRMs) were prepared in the same manner with each batch of unknowns. For carbonate-rich samples, splits of the SRM solutions were spiked with a Ca-Ba-Sr cocktail to matrix-match the igneous rock SRMs to the carbonate unknowns (30–70 wt.% CaO) and bracket anticipated high concentrations of Ba (1000–2000 ppm) and Sr (850–3500 ppm). The following SRMs were used to calibrate the runs: K1919, JA-1, W-2, RGM-1, and AGV-1. Data were reduced by blank subtraction, external drift correction, and standard calibration. Calibrations were strongly linear (R2 > 0.999). Interference corrections were applied to 66Zn (50Ti16O), 69Ga (138Ba++), and 151Eu (135Ba16O). Elements reported as ppm; oxides as wt%; isotopes monitored on ICP-MS given. Average and relative standard deviation are given for SRM AGV and IOBC, which were analyzed as unknowns in the ODP 1149 runs. IOBC values are compared to those obtained by *Plank and Ludden* [1992] by DCP flux fusion (corrected for 9.65% LOI). Note agreement in Zr within uncertainty, demonstrating a lack of zircon in IOBC. Disagreement in IOBC Zn due to volatilization during DCP fusion. Wet bulk density from shipboard index property measurements of closest similar sample [*Plank et al.*, 2000]. This is the density of the in situ sample, including the pore fluid, and is calculated from the bulk volume and total mass of the index sample. Water content is that lost in drying sample to 105°C, from shipboard index property measurements of closest similar sample. Dry bulk density is the ratio of the dry mass (after drying to 105°C) to the total volume of the index sample and is calculated from the product of the wet bulk density and (100-%water content)/100. This density is used to weight the concentration and depth interval of each sample.

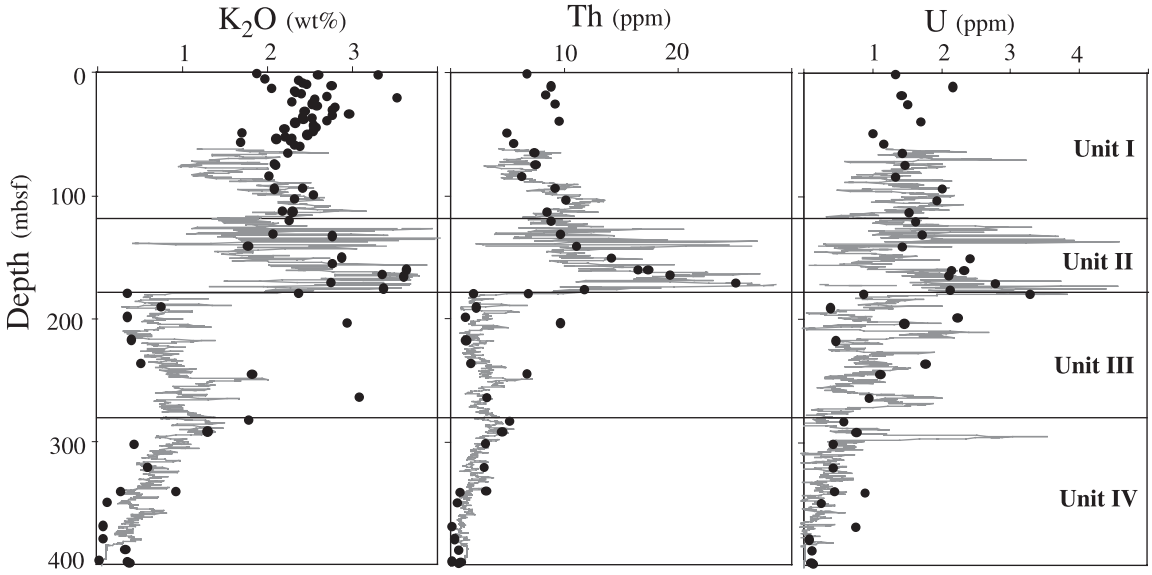


**Figure 3.** Comparison of natural gamma ray logging data to core analyses at ODP 1149. Gray lines are borehole data from hostile environmental gamma ray spectrometry tool, from the triple combo tool string. Symbols are individual core analyses (Tables 1 and 2). Logging data corrected for water content (Table 3), so as to be comparable to core concentrations reported relative to dried powders (at 110°C). Note good correspondence in two data sets, for example, the strong increase in Th toward the base of Unit II and the steady decline in U from Unit III to IV. Unit averages agree well between logging and core data, within 5% for Th, 15% for U, and 17% for $K_2O$ (Table 4).

formation. Details of the corrections are given in Table 3.

## 4. Geochemical Variations in Site 1149 Sediments

[7] The results of the geochemical analyses of the core samples, combined with the logging data, confirm the lithostratigraphic boundaries defined onboard ship (Figure 2). Units I and II are marked by high $Al_2O_3$ typical of clays, and are compositionally homogeneous relative to the units below. The top of Unit III is marked by an abrupt appearance of chert, and uniformly high $SiO_2$ contents recorded in the geochemical logs. Unit IV is defined by the first appearance of biogenic carbonate, which increases in abundance toward the base of the core as the abundance of siliceous lithologies decrease. The core analyses also provide a detailed view of the geochemical variations downcore for tracers useful to the subduction recycling problem, including Ce/Pb, Ba/La, and Ce anomaly (Figure 4).

## 5. Calculating the Bulk Composition of Site 1149 Sediments

[8] The most accurate chemical budgets for sedimentary columns require well-integrated core analyses and logging data [e.g., *Plank and Ludden*, 1992]. This is because while core analyses are highly accurate, they provide a limited sampling of the column (in this case 45–90 samples over 400 m). The logging data, on the other hand, are continuous, but smoothed over ~1 m footprint, and not as accurate as core analyses. Figures 2 and 3 show favorable comparisons between core analyses and $SiO_2$, $Al_2O_3$, CaO, U, Th and K logging data, which help guide the calculation of the Site 1149 bulk compositions. Below are the steps taken to calculate the bulk composition of each unit at Site 1149.

[9] The Unit I bulk composition is the best determined for the site. Although the proportions of ash and clay vary in detail [*Plank et al.*, 2000], there is little overall compositional variation in Unit I. Moreover, 100% of this unit was recovered, and subjected to the greatest number of major element analyses (n = 51; Table 1) The relative standard deviation (RSD) in the elemental concentrations of these Unit 1 samples is <20% with few exceptions, and for some elements approaches analytical precision (e.g., 5% RSD for Al). Thus the bulk composition of Unit I is simply calculated as the mass-weighted mean of the core analyses, where the mass weightings are the product of the dry bulk density and the length of the core represented by each analysis (see Table 2 for values). The average

**Table 3.** Factors Used to Correct Geochemical Logging Data and Natural Gamma Logging Data[a]

| | $Na_2O/Al_2O_3$ | $MgO/Al_2O_3$ | $CaO/Al_2O_3$ | m ($H_2O$+) | b($H_2O$+) | Density (w) | Density (g) |
|---|---|---|---|---|---|---|---|
| Unit I | 0.25 | 0.18 | 0.17 | −0.55 | 42.5 | 1 | 2.8 |
| Unit IIA | 0.13 | 0.18 | 0.05 | −0.55 | 42.5 | 0.95 | 2.45 |
| Unit IIB | 0.13 | 0.18 | 0.05 | −0.55 | 42.5 | 1 | 2.8 |
| Unit III | 0.25 | 0.18 | 0.17 | −0.39 | 39.4 | 0.95 | 2.45 |
| Unit IV | 0.25 | 0.54 | n.a. | −0.39 | 39.4 | 1 | 2.8 |

[a] Corrections to geochemical logging tool (GLT) data: Routine reduction of logging data [e.g., *Pratson*, 2000] normalizes oxides to 100%, making assumptions as to remaining oxides that are not determined (MgO, $Na_2O$, CaO and $H_2O$+, mineral-bound water released >100°C). ICP-ES analyses (Table 1) are used here to accurately estimate MgO, $Na_2O$, and CaO, assuming constant ratios to $Al_2O_3$. GLT $Al_2O_3$ data are multiplied by factors above to determine $Na_2O$, MgO, and CaO. CaO in Unit IV calculated from GLT $CaCO_3$, assuming pure calcite (e.g., CaCO3*0.56). $H_2O$+ abundances estimated differently, since they anticorrelate with $SiO_2$ and $Al_2O_3$. Linear regressions of data within each unit yielded equations for $H_2O$+ as a function of $SiO_2$: $H_2O+ = SiO_2(m) + b$, with m and b given above. Thus MgO, $Na_2O$, and CaO were added to each GLT analysis according to $Al_2O_3$, and $H_2O$+ was added according to $SiO_2$. Analyses were then renormalized to 100%, and $H_2O$+ recalculated from new $SiO_2$, and the process was iterated once more. This procedure generally decreases concentrations of the oxides, and leads to better agreement with the core analyses (Figure 2). Si, Al, and Ca logging data are most reliable; other oxides may be close to detection limits. Corrections to natural gamma data (K, Th, U): Natural gamma data are reported with respect to in situ concentrations, which include the water/porosity of the formation. To enable comparison to the core analyses, which are reported with respect to samples dried at 100°C, logging data were corrected for water contents ($H_2O$-, or wt% water lost between 0–100°C). Density and $H_2O$- are related through mixing of water and its density, with solid material and its grain density, using the relationship $H_2O- = 100*[dens(g)/dens(b) - 1]/[dens(g)/dens(w) - 1]$, where dens(g) is the grain density and dens(w) is the density of formation water, given above, and calculated from the shipboard index measurements for each unit. Dens(b) is the wet bulk density measured in the same logging run as the natural gamma data. Once corrected for $H_2O$-, the K, Th, and U logging data agree well with core measurements (Figure 3).

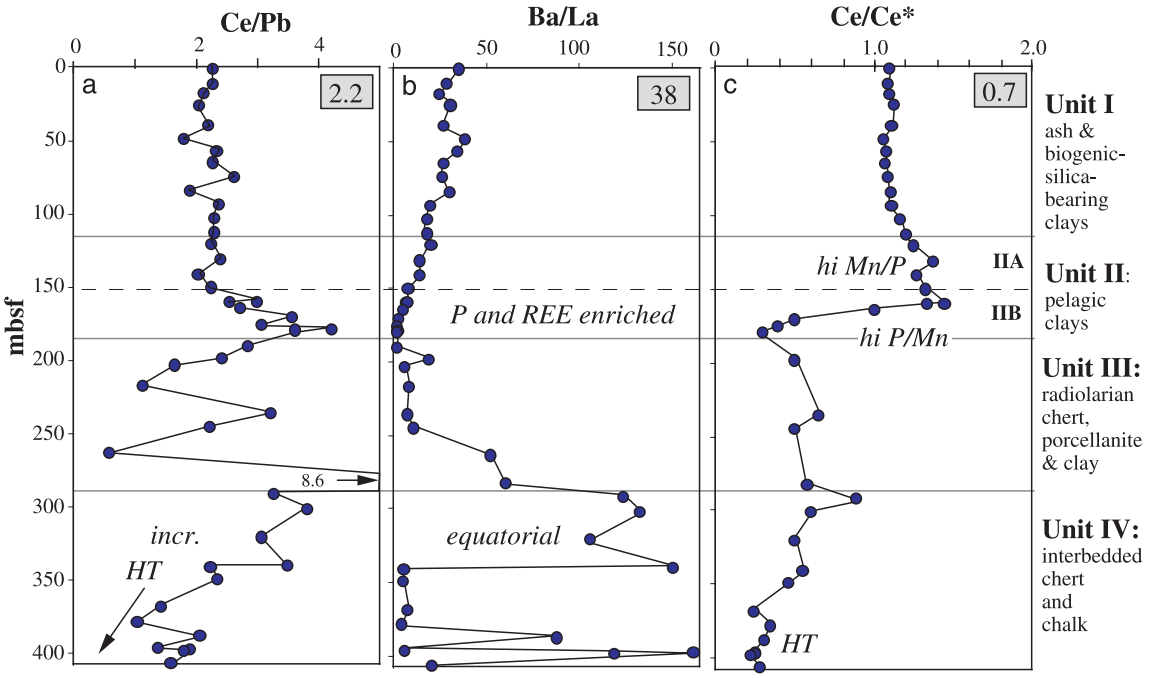


**Figure 4.** Downcore geochemical variations in ODP Site 1149 sediments. Unit I is dominated by arc ash and continentally derived eolian dust (see also Figure 6). The bottom half of Unit II records slow sedimentation rates and high concentrations of fish debris phosphate, which increase the REE (Ce, La). The switch from positive (Ce/Ce* > 1) to negative (Ce/Ce* < 1) Ce anomalies reflects a change in Mn/P, through the scavenging of Ce4+ by Mn-Fe oxyhydroxides, and the uptake of seawater with low Ce/Ce* by fish debris phosphate [*Plank and Langmuir*, 1998]. Ba/La increases dramatically in Unit IV due to high Ba flux accompanying high biological productivity near the equator. Decreases in Ce/Pb and Ce/Ce* at the base of the sedimentary section reflect hydrothermal sediments (HT) near the mid-ocean ridge axis. These tracers are also useful within the subduction zone, as Ce/Pb < 30, Ba/La > 10, and Ce/Ce* < 1 are typical features of most arc basalts [*Elliott*, 2003], including those in the Izu volcanic arc [*Taylor and Nesbitt*, 1998]. Values in gray boxes are bulk site averages from Table 4.

**Table 4.** Bulk Composition of Izu Trench Sediments Based on ODP 1149[a]

| Unit | I | | II | | III | | IV | | Bulk | | |
|---|---|---|---|---|---|---|---|---|---|---|---|
| Thickness, m | 118 | | 61 | | 104 | | 125 | | 408 | | |
| Wet bulk dens. | 1.43 | | 1.47 | | 1.82 | | 2.11 | | 1.74 | | |
| Water, % | 54.2 | | 47.4 | | 22.6 | | 18.2 | | 31.6 | | |
| Dry bulk dens. | 0.653 | | 0.773 | | 1.41 | | 1.73 | | 1.19 | | |
| Mass prop. | 16% | ± | 10% | ± | 30% | ± | 44% | ± | 100% | ± | % |
| $SiO_2$, wt% | **55.68** | 0.72 | **50.68** | 2.3 | **79.94** | 2.40 | **61.28** | 0.61 | **64.98** | 0.77 | 1% |
| $TiO_2$ | **0.614** | 0.043 | **0.627** | 0.1 | **0.240** | 0.02 | **0.132** | 0.02 | **0.289** | 0.01 | 5% |
| $Al_2O_3$ | **14.41** | 0.58 | **15.60** | 1.3 | **3.49** | 0.31 | **2.06** | 0.35 | **5.76** | 0.23 | 4% |
| $Fe_2O_3$(T) | **6.09** | 0.79 | **6.80** | 0.9 | **3.76** | 0.34 | **1.74** | 0.30 | **3.53** | 0.21 | 6% |
| MnO | **0.279** | 0.036 | **1.257** | 0.2 | **0.574** | 0.05 | **0.123** | 0.02 | **0.39** | 0.02 | 6% |
| CaO | **2.06** | 0.27 | **1.14** | 0.2 | **0.54** | 0.05 | **15.84** | 0.32 | **7.63** | 0.14 | 2% |
| MgO | **2.43** | 0.32 | **3.13** | 0.3 | **1.25** | 0.11 | **1.26** | 0.21 | **1.63** | 0.11 | 7% |
| $Na_2O$ | **3.18** | 0.41 | **2.40** | 0.4 | **1.00** | 0.09 | **0.38** | 0.06 | **1.20** | 0.08 | 6% |
| $K_2O$ | **2.25** | 0.29 | **2.67** | 0.2 | **0.95** | 0.09 | **0.57** | 0.10 | **1.16** | 0.07 | 6% |
| $P_2O_5$ | **0.100** | 0.013 | **0.475** | 0.1 | **0.206** | 0.02 | **0.055** | 0.01 | **0.15** | 0.01 | 6% |
| $CO_2$ | **0** | | **0** | | **0** | | **10.1** | | **4.49** | 0.40 | 9% |
| $H_2O$ | **12.26** | 1.59 | **15.11** | 2.3 | **8.78** | 0.79 | **6.05** | 2.75 | **8.73** | 0.81 | 9% |
| Sum | 99.34 | | 99.87 | | 100.74 | | 99.62 | | 99.94 | | |
| Li, ppm | **42.4** | 5.5 | **62.7** | 9.4 | **27.1** | 2.44 | **58.9** | 10.02 | **47.1** | 4.46 | 9% |
| Be | **1.75** | 0.23 | **2.53** | 0.3 | **0.96** | 0.09 | **0.74** | 0.12 | **1.14** | 0.07 | 6% |
| Sc | **18.6** | 2.1 | **24.1** | 3.6 | **7.3** | 0.66 | **4.01** | 0.68 | **9.26** | 0.56 | 6% |
| V | **122** | 16 | **123** | 18.5 | **52** | 4.72 | **19** | 3.29 | **55.7** | 3.41 | 6% |
| Cr | **49.5** | 6.4 | **52.3** | 7.9 | **39.6** | 3.56 | **9.9** | 1.69 | **29.2** | 1.69 | 6% |
| Co | **21.9** | 2.9 | **108.0** | 16.2 | **12.3** | 1.10 | **6.5** | 1.10 | **20.5** | 1.62 | 8% |
| Ni | **46.4** | 6.0 | **203.4** | 30.5 | **53.0** | 4.77 | **20.9** | 3.55 | **52.3** | 3.49 | 7% |
| Cu | **106** | 14 | **211** | 31.6 | **134** | 12.03 | **48** | 8.22 | **99.0** | 5.95 | 6% |
| Zn | **94.7** | 4.7 | **127.2** | 19.1 | **76.4** | 6.88 | **49.9** | 8.48 | **72.5** | 4.47 | 6% |
| Ga | **17.4** | 1.1 | **19.1** | 2.4 | **6.4** | 0.57 | **9.6** | 1.62 | **10.8** | 0.75 | 7% |
| Rb | **90.8** | 12 | **112.9** | 16.9 | **33.4** | 3.00 | **24.7** | 4.19 | **46.3** | 3.01 | 7% |
| Sr | **138** | 12 | **156** | 23.3 | **85** | 7.61 | **165** | 28.10 | **136** | 12 | 9% |
| Y | **26.8** | 3.5 | **96.9** | 14.5 | **35.4** | 3.18 | **16.6** | 2.82 | **31.6** | 2.03 | 6% |
| Zr | **90.6** | 7.4 | **130.9** | 19.6 | **48.8** | 4.40 | **30.6** | 5.21 | **55.3** | 3.24 | 6% |
| Nb | **8.4** | 1.1 | **11.7** | 1.8 | **4.3** | 0.38 | **3.3** | 0.57 | **5.22** | 0.34 | 7% |
| Cs | **7.1** | 0.92 | **9.3** | 1.4 | **1.7** | 0.15 | **1.1** | 0.18 | **3.00** | 0.20 | 7% |
| Ba | **568** | 73 | **398** | 35 | **255** | 23 | **1531** | 260 | **884** | 111 | 13% |
| La | **21.2** | 2.8 | **62.4** | 9.4 | **26.2** | 2.35 | **13.8** | 2.34 | **23.4** | 1.50 | 6% |
| Ce | **50.1** | 6.5 | **118.1** | 17.7 | **28.2** | 2.54 | **14.5** | 2.46 | **34.3** | 2.23 | 6% |
| Pr | **5.60** | 0.73 | **19.11** | 2.9 | **6.38** | 0.57 | **3.37** | 0.57 | **6.16** | 0.40 | 7% |
| Nd | **21.7** | 2.8 | **79.4** | 11.9 | **26.1** | 2.34 | **14.0** | 2.38 | **25.2** | 1.65 | 7% |
| Sm | **4.76** | 0.62 | **18.20** | 2.7 | **5.36** | 0.48 | **2.69** | 0.46 | **5.32** | 0.35 | 7% |
| Eu | **1.22** | 0.16 | **4.28** | 0.6 | **1.30** | 0.12 | **0.76** | 0.13 | **1.34** | 0.09 | 7% |
| Gd | **4.79** | 0.62 | **19.20** | 2.9 | **5.87** | 0.53 | **2.86** | 0.49 | **5.66** | 0.37 | 7% |
| Tb | **0.786** | 0.10 | **3.050** | 0.5 | **0.905** | 0.08 | **0.431** | 0.07 | **0.88** | 0.06 | 7% |
| Dy | **4.61** | 0.60 | **17.60** | 2.6 | **5.23** | 0.47 | **2.48** | 0.42 | **5.11** | 0.33 | 7% |
| Ho | **0.95** | 0.12 | **3.54** | 0.5 | **1.08** | 0.10 | **0.50** | 0.08 | **1.04** | 0.07 | 6% |
| Er | **2.68** | 0.35 | **9.60** | 1.4 | **2.90** | 0.26 | **1.32** | 0.22 | **2.82** | 0.18 | 6% |
| Yb | **2.67** | 0.35 | **8.49** | 1.3 | **2.57** | 0.23 | **1.15** | 0.20 | **2.53** | 0.16 | 6% |
| Lu | **0.417** | 0.054 | **1.302** | 0.2 | **0.396** | 0.04 | **0.173** | 0.03 | **0.39** | 0.02 | 6% |
| Hf | **2.63** | 0.20 | **3.89** | 0.6 | **1.09** | 0.10 | **0.72** | 0.12 | **1.44** | 0.08 | 6% |
| Ta | **0.630** | 0.082 | **0.876** | 0.1 | **0.267** | 0.02 | **0.211** | 0.04 | **0.359** | 0.02 | 7% |
| Pb | **22.6** | 2.9 | **44.2** | 6.6 | **18.2** | 1.64 | **4.6** | 0.78 | **15.4** | 0.92 | 6% |
| Th | **7.93** | 0.24 | **14.40** | 0.7 | **2.74** | 0.08 | **2.06** | 0.02 | **4.39** | 0.08 | 2% |
| U | **1.55** | 0.06 | **2.02** | 0.3 | **0.94** | 0.01 | **0.44** | 0.05 | **0.92** | 0.04 | 4% |
| $^{206}Pb/^{204}Pb$ | **18.607** | 0.024 | **18.614** | 0.0064 | **18.618** | 0.2956 | **18.430** | 0.0715 | **18.589** | 0.103 | |
| $^{207}Pb/^{204}Pb$ | **15.613** | 0.0016 | **15.618** | 0.0078 | **15.565** | 0.0511 | **15.534** | 0.0092 | **15.587** | 0.018 | |
| $^{208}Pb/^{204}Pb$ | **38.723** | 0.011 | **38.758** | 0.0378 | **38.419** | 0.2000 | **38.223** | 0.1164 | **38.558** | 0.071 | |
| $^{87}Sr/^{86}Sr$ | **0.70962** | 0.0023 | **0.71198** | 0.0003 | **0.71307** | 0.0012 | **0.70782** | 0.0004 | **0.70956** | 0.00045 | |
| $^{143}Nd/^{144}Nd$ | **0.51240** | 9.3E-05 | **0.51232** | 7.1E-06 | **0.51228** | 2.8E-05 | **0.51228** | 3.0E-05 | **0.51231** | 0.00002 | |

**Table 4.** (continued)

| Unit | I | | II | | III | | IV | | Bulk | | |
|---|---|---|---|---|---|---|---|---|---|---|---|
| Thickness, m | **118** | | **61** | | **104** | | **125** | | **408** | | |
| Wet bulk dens. | **1.43** | | **1.47** | | **1.82** | | **2.11** | | **1.74** | | |
| Water, % | **54.2** | | **47.4** | | **22.6** | | **18.2** | | **31.6** | | |
| Dry bulk dens. | **0.653** | | **0.773** | | **1.41** | | **1.73** | | **1.19** | | |
| Mass prop. | **16%** | ± | **10%** | ± | **30%** | ± | **44%** | ± | **100%** | ± | % |
| Natural gamma log estimates, % diff | | | | | | | | | | | |
| $K_2O$, wt% | **1.95** | −13% | **2.44** | −9% | **0.87** | −9% | **0.67** | 17% | **1.10** | | |
| Th, ppm | **8.15** | 3% | **13.7** | −5% | **2.83** | 3% | **2.05** | −1% | **4.38** | | |
| U, ppm | **1.49** | −4% | **1.71** | −15% | **0.93** | −1% | **0.38** | −12% | **0.85** | | |
| Geochemical log estimates, % diff | | | | | | | | | | | |
| $SiO_2$ | **54.96** | −1.3% | **n.d.** | n.d. | **81.99** | 3% | **61.98** | 1% | | | |
| $Fe_2O_3$ | **2.62** | −57.0% | **n.d.** | n.d. | **3.78** | 1% | **2.13** | 22% | | | |
| $TiO_2$ | **1.48** | 141.3% | **n.d.** | n.d. | **0.34** | 42% | **0.15** | 16% | | | |
| $K_2O$ | **1.69** | −24.8% | **n.d.** | n.d. | **0.80** | −16% | **0.67** | 17% | | | |
| $Al_2O_3$ | **17.73** | 23.1% | **n.d.** | n.d. | **4.14** | 19% | **2.43** | 18% | | | |
| CaO | **2.96** | 43.8% | **n.d.** | n.d. | **0.69** | 27% | **16.17** | 2% | | | |
| Opal | **11** | | **0** | | **66** | | **50** | | **44** | | |
| Calcite | **0** | | **0** | | **0** | | **23** | | **10** | | |
| Terrigenous | **89** | | **100** | | **34** | | **27** | | **46** | | |

[a] Bulk averages calculated from core data in Table s 1and 2; logging data corrected as in Table 3 and as outlined in the text. Density and water content from index properties measured in core samples [*Plank et al.*, 2000] for Units I and II, and from logging measurements for Units III and IV (as corrected in Table 3). $CO_2$ calculated from data of *Sadofsky and Bebout* [2004] or from assuming all CaO as $CaCO_3$. Isotopic ratios are averages and standard deviations of the data of *Hauff et al.* [2003] within each unit. The isotopic data for sample 1149B-16R-1–93 were excluded from Unit IV average because they are dominated by volcanic inputs not typical of the unit. Uncertainties on the unit means derive from the logging data for $K_2O$, Th, U, and $SiO_2$. For all other elements, uncertainty is the maximum of the natural gamma logs (e.g., 13% for Unit I), or %RSD of the core analyses, whichever is smaller. Uncertainty on the bulk site mean derives from a Monte Carlo scheme, where each unit is allowed to vary within its uncertainty to calculate a weighted mean for the site. The uncertainty reported is the maximum difference of these means from the reported bulk, for 90 out of the 100 trials.

is based on the 13 analyses with complete major and trace elements (Table 2), but is very similar (<3% relative) to that calculated from the fuller data set for the major elements. The natural gamma logs strongly corroborate this bulk composition, and provide support for both the averaging method, and the accuracy of the logging data. Even though logging data were only collected for the lower half of this unit, the simple averages of the natural gamma logging concentrations agree within 3% (for Th) to 13% (for $K_2O$) of the weighted mean of the core analyses (Table 4). The geochemical logs are in general less accurate than the natural gamma logs, with the exception of $SiO_2$, where the logging average (55.0 wt% $SiO_2$) is within ~1% relative of the core average (55.7 wt% $SiO_2$). The Sr, Nd and Pb isotopic compositions for each unit are calculated from the isotopic data of *Hauff et al.* [2003] (details given in Table 4).

[10] The bulk composition of Unit II has greater inherent uncertainties than that for Unit I, due to the wider compositional variability (particularly IIB clays), and the lack of geochemical logging data due to hole constriction. The mass-weighted average of the nine core analyses is slightly higher in Th, U and $K_2O$ than the logging averages, from 5% for Th to 15% for U (Table 4). These small differences may be attributed to nonrepresentative sampling, poor hole conditions in this interval, or to the fact that coring occurred in Hole A while logging occurred in Hole B.

[11] Unit III consists of chert-rich and clay-rich layers, and drilling recovery was low (3%). Core samples thus may not be representative of the site, and are likely to be biased by the lithology preferentially recovered. Indeed, the simple weighted mean of the nine core analyses are lower in $SiO_2$ and greater in U, Th and K than the logging estimates, consistent with an oversampling of soft clay-rich material in the core analyses. Because the logging data are more continuous, and our previous tests demonstrate their accuracy (e.g., 1% relative accuracy for $SiO_2$ in Unit I; Table 4), we correct the mean of the core samples to the mean of the logging data by adding 20% additional chert (using the composition of the lowest Al sample, 1149B-9R-1-26, for the chert component). This adjusted composition agrees with the logging averages by a few percent for Th, U and $SiO_2$ (Table 4).

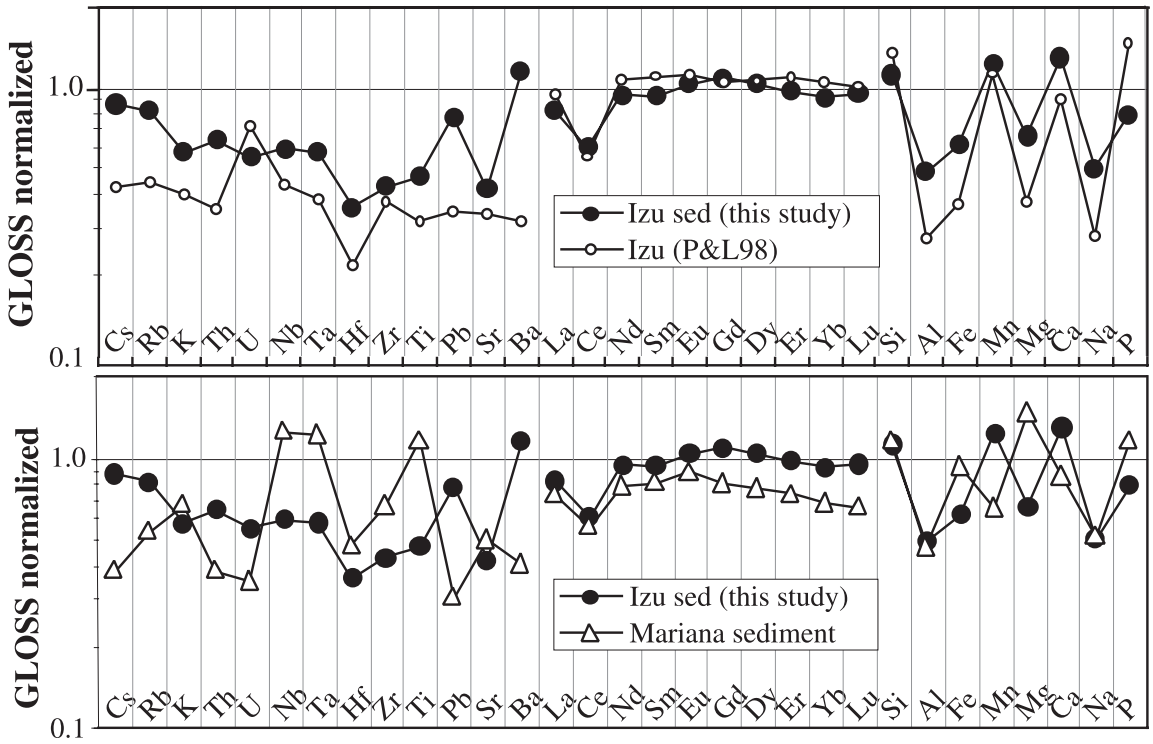


**Figure 5.** Bulk estimates for Izu and Mariana trench sediments, normalized to global subducting sediment average (GLOSS). (top) Comparison of Izu estimate from this study (Table 4) to previous estimate made without the benefit of a reference drill site within 1000 km. (bottom) Comparison of Izu sediment to Marianas sediment. GLOSS, previous Izu sediment, and Marianas sediment from *Plank and Langmuir* [1998].

[12] Like Unit III, Unit IV was poorly recovered (10%) and includes lithologies of vastly different compositions (chert and chalk). Thus we rely again on the logging data to guide the averaging of the core samples. The simple weighted mean of the 14 core analyses in Unit IV leads to remarkably similar logging average for $SiO_2$ and CaO (highly sensitive to end-member chert and chalk proportions), but appears to underestimate K and Th. We thus compensate by adding 20% of a clayey-marl (1149B-22R-1-20), which raises trace elements without having a major effect on silica or calcium. This corrected composition brings K and U within 15% of the logging average, while still keeping Th, Si and Ca within 1–2% (Table 4).

[13] The bulk composition of Site 1149 sediments can now be calculated from the chemical compositions and mass proportions of the four units. It is important to note that the while Units III and IV make up roughly half of the site by thickness, they make up almost 75% of the site by mass, and so have a large effect on the mass-weighted bulk composition of the site. This is not an artifact of our core adjustments (above) but is observed in both the core and logging density measurements, reflecting the greater compaction of clays deeper in the core, and the greater grain density of chert and carbonate lithologies. The mass-weighted mean composition for the site is given in Table 4, with uncertainties in the bulk composition calculated from uncertainties for each unit using a Monte Carlo method (Table 4). The errors on the bulk composition for all elements are less than 10% of their values, except Ba (13%), due to its high variability and concentration within Unit IV (i.e., 10–2800 ppm Ba). Even so, the bulk composition of the site is constrained remarkably well, due to the 45 well-chosen core samples and the utility of the logging data.

## 6. Comparison of Izu Bulk Sediment to Other Sediment Averages

[14] It is useful to compare the Site 1149 Izu sediment average here with the compilation of *Plank and Langmuir* [1998] (hereinafter "P&L98"), which includes estimates for the Izu and Marianas trenches, as well as global subducting sediment (GLOSS). The P&L98 Izu trench average was based on the pelagic sections drilled

at Site 800 (~1000 km to the south), since at the time there were no complete drilled sections seaward of Izu. Extra chert was added to make up for the inferred greater thickness of sediment. At Site 1149, a thinner sedimentary section was drilled (470 m) than initially estimated (600 m), and a top unit of volcanic ash-bearing diatom/radiolarian clay was encountered that was not included in the P&L98 estimate. Figure 5 compares the two Izu sediment estimates, normalized to GLOSS. The previous estimate is overdiluted by ~40% due to the chert added to make up the inferred extra thickness of the site, and the misfits in silica and alkalis are quantitatively consistent with 40% extra chert. On the other hand, the previous Izu estimate is overenriched in U, Mn, P and REE, due to the overabundance of red clay assumed (similar to Unit IIB at Site 1149) and the lack of ash-bearing sediment similar to Unit I. Thus the misfits in the previous Izu average result largely from the differences in the lithologic units and thicknesses that were assumed in the absence of drilling. Clearly, the average in Table 4 is more accurate than the estimates in P&L98.

[15] The Izu sediment average here also supersedes other previously published estimates. A preliminary average was published by *Straub et al.* [2004], based on our data and a simple averaging of analyses within each unit. The main difference in this preliminary estimate is its overweighting of the clay fraction in Unit III, leading to lower Th/La and higher Th/U, Nd/Hf and $^{206}Pb/^{204}Pb$ than the better constrained Izu sediment average in Table 4. *Hochstaedter et al.* [2000] also present an average Izu sediment composition, based on three samples from DSDP 195 and 198 sediments, which they average in the proportion of 50% clay (2 samples) to 50% chalk (1 sample). Their clay samples are similar to Unit IIB at Site 1149 (~150–180 mbsf), and so their average is strongly biased to REE-rich pelagic clays. In addition to omitting the chert, their average also lacks Ba-rich sediments as found in the base of Site 1149. Thus their average contrasts greatly with the Site 1149 sediment average in Table 4, with strong excesses in REE relative to Th, Pb and Ba. Their Pb isotopic values are also much more radiogenic than the measurements in *Hauff et al.* [2003] of Site 1149 sediments.

[16] *Hauff et al.* [2003] focus on bulk estimates for Sr, Nd and Pb isotopes at Site 1149. Because they use our concentration data, and we use their isotope data, our estimates should be similar. Indeed, the isotopic averages of *Hauff et al.* [2003] are generally within the uncertainties estimated here, because we averaged the same 10 isotopic analyses, albeit with different weighting factors. Our elemental concentrations (Table 4) differ from those calculated by *Hauff et al.* [2003], however, which are 40% higher for Sr, 80% higher for Nd and 17% higher for Pb. The differences derive from *Hauff et al.* [2003] using only the 10 samples they analyzed isotopically to estimate elemental concentrations for the site, since the isotopic systems were the focus of their work. These 10 samples are not entirely representative of the site, and lead to an overweighting of carbonate in Unit IV (and hence high Sr) and of REE-rich clay in Unit IIB (and hence the high Nd). Given the larger number of analyses and logging data used here, we recommend the values in Table 4 as the most robust averages for Site 1149 sediments.

[17] The Site 1149 bulk composition differs from GLOSS in several ways (Figure 5). GLOSS is dominated by terrigenous material typical of upper continental crust, due to the large volume of terrigenous sediments at continental margins that dominate the global average. Thus the biogenic siliceous and carbonate lithologies in Units III and IV at Site 1149 lead to large (~50%) dilution relative to GLOSS for those elements dominated by terrigenous inputs (e.g., K, Th, U, Nb, Zr, Ti, and Al). This observation is consistent with quantitative estimates of the proportion of calcium carbonate, opal and clay at the site. Assuming all the $CO_2$ exists as pure $CaCO_3$, and all the $SiO_2$ in excess of 51 wt% (the average of the opal-absent pelagic clays in Unit II) exists as biogenic opal (with 95 wt% $SiO_2$), then the Site 1149 average sediment contains 10 wt% $CaCO_3$, 44 wt% opal, and 46 wt% terrigenous material. Thus the ~50% dilution of terrigenous material is expected, as is the enrichment in elements associated with the biogenic carbonate (Ca) and opal (Si and Ba). Somewhat unexpected is the depleted Sr in the carbonate-rich Izu sediment relative to GLOSS; this is due to the low Sr abundances in Izu carbonate (<500 ppm), which is typical of Cretaceous carbonates [*Baker et al.*, 1982; *Renard et al.*, 1983]. The relatively high abundances of REE, Mn, and Pb, and the large negative Ce anomaly in Site 1149 relative to GLOSS, reflect the hydrogenous, hydrothermal and biogenic phosphate inputs to Unit II–IV sediments (cf. P&L98). One notable feature of the Izu sediments with respect to GLOSS is high Cs/K, which may reflect input of highly

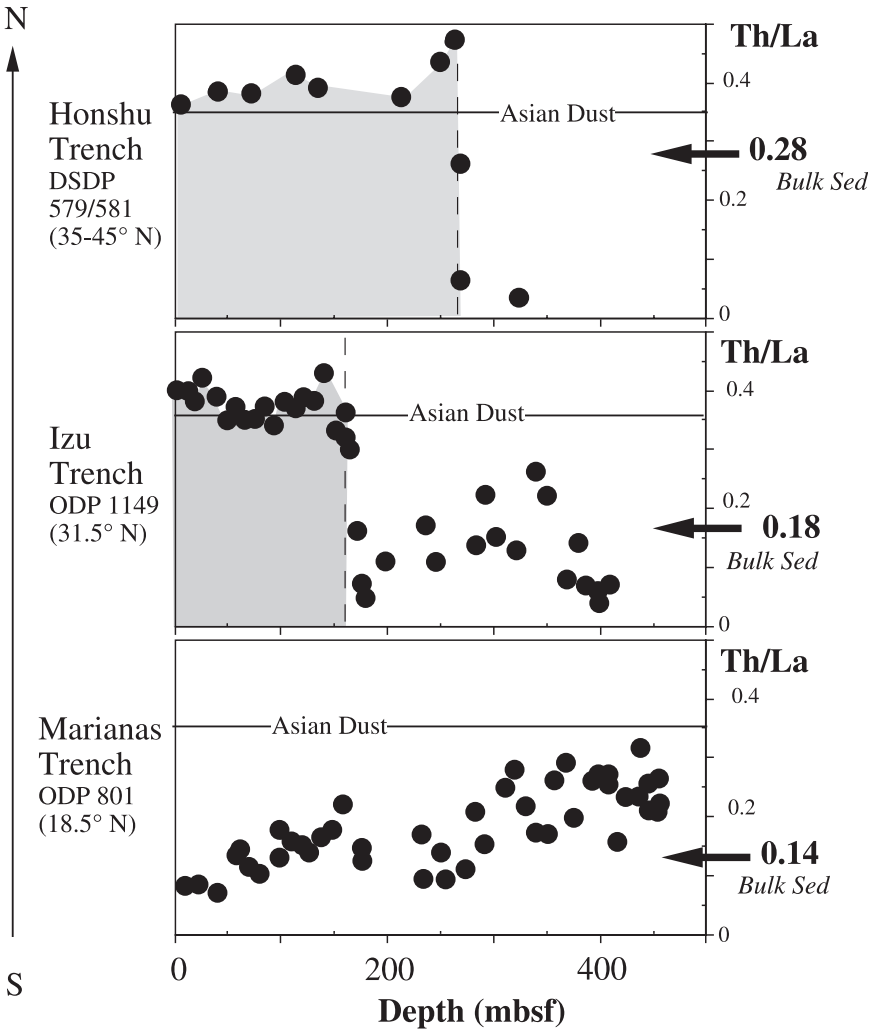


**Figure 6.** Variation in Th/La in sedimentary columns entering Mariana, Izu and Honshu trenches. Sections ordered north to south, to emphasize the appearance of upper continentally derived eolian unit that appears when sites cross into the westerly wind belt (north of ~20°N). This eolian unit has compositions similar to Asian dust and notably high Th/La, which is a feature of the upper continental crust [*Plank*, 2005]. The thickening of this unit northward leads to an increase in Th/La in the bulk sediment. This latitudinal signal along-strike of the Mariana-Izu-Bonin-Honshu trench leads to a sympathetic northward increase in Th/La of the volcanic arcs (see Figure 7). Data sources: Mariana sediment data [*Karl et al.*, 1992]; Izu sediment data (Table 2); Honshu sediment data [*Cousens et al.*, 1994]; bulk sediment estimates [*Plank and Langmuir*, 1998] (Table 4); Asian dust [*Jahn et al.*, 2001].

weathered sources (which retain Cs > Rb > K [*McLennan et al.*, 1990; *McLennan*, 2001]).

[18] The final important comparison is between the sediments feeding the Izu versus Mariana trenches (Figure 5). Both regions contain red clays and abundant cherts, but the more northerly Izu site contains an ash and Asian dust-rich unit at its top [*Urbat and Pletsch*, 2003] which is absent to the south, while the Marianas sites contain Cretaceous volcaniclastics absent to the north. The low Cs/K, Th and U in the Marianas sediments derive directly from these ocean-island type volcanic sources [*Lancelot et al.*, 1990; P&L98]. The enrichment of Nb, Ta and Ti, as well as the depletion in the HREE in the Marianas sediment, are other unique features of OIB-type volcaniclastics. Thus most of the geochemical differences in the sediments entering the two trenches can be traced to volcanic versus continental sources of material. The 10% biogenic carbonate at Site 1149 has a minor effect, leading to the expected Ca enrichment, but little effect on Sr (as noted above). The enrichment in Ba

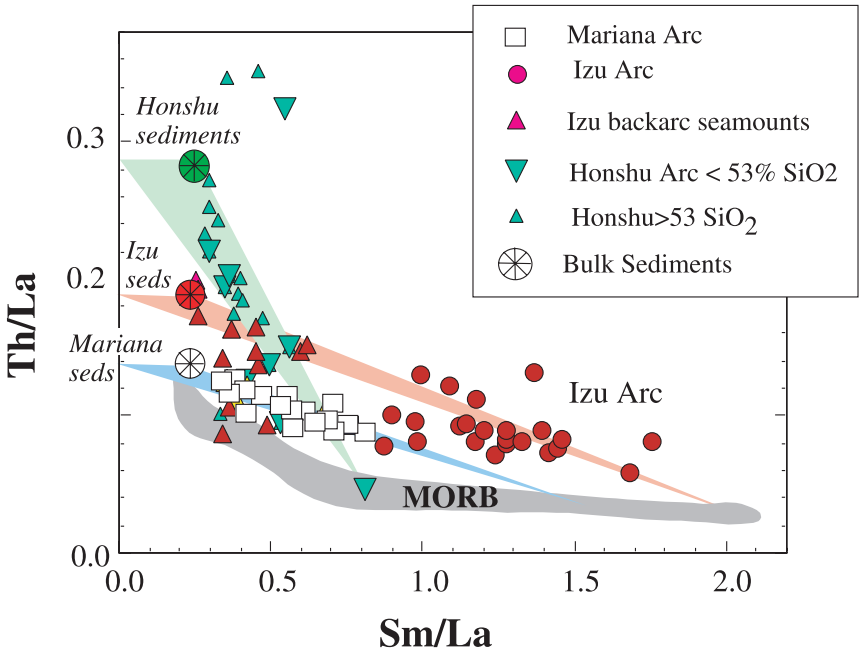


**Figure 7.** Th/La and Sm/La in arc volcanics show mixing toward local sediments [see also *Plank*, 2005]. Each arc forms a mixing trend between a mantle composition (in the MORB array) and a sedimentary composition, which in each case has similar Th/La to the nearby trench sediment. These western Pacific arcs also show systematic regional trends, where arcs mix toward bulk sediment with progressively higher Th/La to the north (Mariana to Honshu), as predicted in Figure 6. Shaded fields drawn from bulk sediment (including variable Sm/La fractionation) through arc sample with lowest Th/La. Arc data from *Elliott et al.* [1997], *Gust et al.* [1995], *Taylor and Nesbitt* [1998], and *Hochstaedter et al.* [2000].

in Izu sediments derives from high abundances in Unit IV at Site 1149 (Ba is commonly over 2000 ppm) which is absent from the Marianas sites (Ba is rarely higher than 500 ppm).

## 7. Using the Izu Sediment to Address Subduction Recycling

[19] Although it represents a single location, Site 1149 provides samples of the dominant sediments subducting along the Izu trench. Seismic reflection transects extend regionally the geochemical information obtained at a single site. The units drilled at Site 1149 show excellent correspondence to the acoustic stratigraphy [*Abrams*, 2002], especially the top chert (Unit II/III), which forms a strong reflector that can be mapped for thousands of kilometers in the western Pacific [*Ewing et al.*, 1968; *Abrams*, 2002]. Likewise, the Cretaceous volcaniclastic layer present seaward of the Mariana Trench can be traced seismically across the Pigafetta Basin [*Abrams et al.*, 1992], but disappears to the north as the number of seamounts wanes. At the same time, an upper layer of continentally derived eolian material thickens to the north, into the westerly wind belt. Drill sites (ODP 800, 801, 1149, 1179, and DSDP 579, and 581) support this regional stratigraphy.

[20] The bulk composition presented here for Izu trench sediments is also useful to understanding the source of Izu arc volcanics, as sediments are subducted, dehydrated and melted, and components from them are incorporated in the source of magmas. While the magnitude of sediment recycling is notably low at the Izu arc [*Taylor and Nesbitt*, 1998; *Straub et al.*, 2004], subducted sediments nonetheless contribute to certain aspects of the geochemical composition of volcanics from the Izu arc and back-arc. For example, the Pb isotopic composition of the lower half of the Izu sediment column is identical to that of the Izu arc [*Hauff et al.*, 2003], and the bulk sedimentary section is an adequate mixing end-member for both the Izu arc and back arc [*Hauff et al.*, 2003; *Straub et al.*, 2004; *Ishizuka et al.*, 2003]. Izu arc basalts also mix toward the sediment Th/La, as predicted from global [*Plank*, 2005] and regional [*Ludden et al.*, 2006] considerations. The bulk Th/La in Western

Pacific sediments increases from south to north, as low Th/La volcaniclastics seaward of the Marianas are replaced by high Th/La, continentally derived eolian material seaward of Izu and Honshu (Figure 6). This along-strike increase in Th/La of the input is mirrored in an along-strike increase in Th/La of the volcanic output (Figure 7). Other predictions, such as a decrease in the negative Ce anomaly and an increase in Cs/K of the bulk sediment to the north (Figure 4c), can be tested in the future against high quality trace element data for IBM volcanics. The sediment compositions presented here thus enable tracer experiments through the subduction zone, and ultimately, mass balance of the input and output through the Izu-Bonin-Mariana subduction factory.

## Acknowledgments

[21] Thanks to the shipboard science party and crew of the JOIDES *Resolution*, during ODP Leg 185. Careful reviews by Jim Gill, Bob Stern, Folkmar Hauff, Gray Bebout, and Valerie Chavagnac helped to improve the manuscript. We are grateful for support from the Joint Oceanographic Institutions, U.S. Science Support Program, and the National Science Foundation (OCE-0136855, OCE-0001897, and EAR-0233712).

## References

Abrams, L. J. (2002), Correlation between core, logging, and seismic data at Site 1149 in the Nadezhda Basin [online], *Proc. Ocean Drill. Program Sci. Results*, *185*, 14 pp. (Available at http://www-odp.tamu.edu/publications/185_SR)

Abrams, L. J., R. L. Larson, T. H. Shipley, and Y. Lancelot (1992), The seismic stratigraphy and sedimentary history of the East Mariana and Pigafetta basins of the western Pacific, *Proc. Ocean Drill. Program Sci. Results*, *129*, 551–569.

Baker, P. A., J. M. Gieskes, and H. Elderfield (1982), Diagenesis of carbonate in deep-sea sediments — Evidence from Sr/Ca ratios and interstitial dissolved Sr data, *J. Sediment. Petrol.*, *52*, 71–82.

Bartolini, A. (2003), Cretaceous radiolarian biochronology and carbon isotope stratigraphy of ODP Site 1149 (northwestern Pacific, Nadezhda Basin) [online], *Proc. Ocean Drill. Program Sci. Results*, *185*, 17 pp. (Available at http://www-odp.tamu.edu/publications/185_SR)

Chauvel, C., E. Lewin, M. Carpentier, and J. Marini (2006), Recycled oceanic material controls the Hf-Nd OIB array, *Eos Trans. AGU*, *87*(52), Fall Meet. Suppl., Abstract U14B-07.

Cousens, B. L., J. F. Allan, and M. P. Gorton (1994), Subduction-modified pelagic sediments as the enriched component in back-arc basalts from the Japan Sea: Ocean Drilling Program Sites 797 and 794, *Contrib. Mineral. Petrol.*, *117*, 421–434.

Elliott, T. R. (2003), Tracers of the slab, in *Inside the Subduction Factory*, *Geophys. Monogr. Ser.*, vol. 138, edited by J. Eiler, pp. 23–45, AGU, Washington, D. C.

Elliott, T., T. Plank, A. Zindler, W. White, and B. Bourdon (1997), Element transport from subducted slab to volcanic front at the Mariana arc, *J. Geophys. Res.*, *102*, 14,991–15,019.

Ewing, J., M. Ewing, T. Aitken, and W. J. Ludwig (1968), North Pacific sediment layers measured by seismic profiling, in *The Crust and Upper Mantle of the Pacific Area*, *Geophys. Monogr. Ser.*, vol. 12, edited by L. Knopoff, C. L. Drake, and P. J. Hart, pp. 147–173, AGU, Washington, D. C.

Gust, D. A., R. J. Arculus, and A. B. Kersting (1995), Aspects of magma sources and processes in the Honshu arc, *Can. Mineral.*, *35*, 347–365.

Hauff, F., K. Hoernle, and A. Schmidt (2003), Sr-Nd-Pb composition of Mesozoic Pacific oceanic crust (Site 1149 and 801, ODP Leg 185): Implications for alteration of ocean crust and the input into the Izu-Bonin-Mariana subduction system, *Geochem. Geophys. Geosyst.*, *4*(8), 8913, doi:10.1029/2002GC000421.

Hochstaedter, A. G., J. B. Gill, B. Taylor, O. Ishizuka, M. Yuasa, and S. Morita (2000), Across-arc geochemical trends in the Izu Bonin arc: Constraints on source composition and mantle melting, *J. Geophys. Res.*, *105*, 495–512.

Ishizuka, O., R. N. Taylor, J. A. Milton, and R. W. Nesbitt (2003), Fluid-mantle interaction in an intra-oceanic arc: Constraints from high-precision Pb isotopes, *Earth Planet. Sci. Lett.*, *211*, 221–236.

Jahn, B., S. Gallet, and J. Han (2001), Geochemistry of the Xining, Xifeng and Jixian sections, loess plateau of China: Eolian dust provenance and paleosol evolution during the last 140 ka, *Chem. Geol.*, *178*, 71–94.

Karl, S. M., G. A. Wandless, and A. M. Karpoff (1992), Sedimentological and geochemical characteristics of ODP Leg 129 siliceous deposits, *Proc. Ocean Drill. Program Sci. Results*, *129*, 31–80.

Kelley, K. A., T. Plank, J. Ludden, and H. Staudigel (2003), Composition of altered oceanic crust at ODP Sites 801 and 1149, *Geochem. Geophys. Geosyst.*, *4*(6), 8910, doi:10.1029/2002GC000435.

Lancelot, Y., et al. (1990), *Proceedings of the Ocean Drilling Program, Initial Reports*, vol. 129, Ocean Drill. Program, College Station, Tex.

Ludden, J. N., T. Plank, R. L. Larson, and C. Escutia (2006), Leg 185 synthesis: Sampling the oldest crust in the ocean basins to understand Earth's geodynamic and geochemical fluxes [online], *Proc. Ocean Drill. Program Sci. Results*, *185*, 35 pp. (Available at http://www-odp.tamu.edu/publications/185_SR)

McLennan, S. M. (2001), Relationships between the trace element composition of sedimentary rocks and upper continental crust, *Geochem. Geophys. Geosyst.*, *2*(4), doi:10.1029/2000GC000109.

McLennan, S. M., S. R. Taylor, M. T. McCulloch, and J. B. Maynard (1990), Geochemical and Nd-Sr isotopic composition of deepsea turbidites: Crustal evolution and plate tectonic associations, *Geochim. Cosmochim. Acta*, *54*, 2015–2050.

Plank, T. (2005), Constraints from thorium/lanthanum on sediment recycling at subduction zones and the evolution of the continents, *J. Petrol.*, *46*, 921–944.

Plank, T., and C. H. Langmuir (1998), The chemical composition of subducting sediment and its consequences for the crust and mantle, *Chem. Geol.*, *145*, 325–394.

Plank, T., and J. N. Ludden (1992), Geochemistry of sediments in the Argo Abyssal Plain at Site 765: A continental margin reference section for sediment recycling in subduction zones, *Proc. Ocean Drill. Program Sci. Results*, *123*, 167–189.

Plank, T., et al. (2000), *Proceedings of the Ocean Drilling Program, Initial Reports* [online], vol. 185, Ocean Drill. Program, College Station, Tex. (Available at http://www-odp.tamu.edu/publications/185_IR/185ir.htm)

Pratson, E. L. (2000), Leg 185: Geochemical processing report, in *Proceedings of the Ocean Drilling Program, Initial Reports* [CD-ROM], vol. 185, Ocean Drill. Program, College Station, Tex.

Renard, M., G. Richebois, and R. Letolle (1983), Trace element and stable isotope geochemistry of Paleocene to Coniacian carbonate samples from Hole 516F, comparison with North Atlantic and Tethys sites, *Initial Rep. Deep Sea Drill. Proj.*, *72*, 399–420.

Rouxel, O., J. Ludden, J. Carignan, L. Marin, and Y. Fouquet (2002), Natural variations of Se isotopic composition determined by hydride generation multiple collector inductively coupled plasma mass spectrometry, *Geochim. Cosmochim. Acta*, *66*, 3191–3199.

Rouxel, O., et al. (2003a), Iron isotope fractionation during oceanic crust alteration, *Chem. Geol.*, *202*, 155–182.

Rouxel, O., J. Ludden, and Y. Fouquet (2003b), Antimony isotope variations in natural systems and implications for their use as geochemical tracers, *Chem. Geol.*, *200*, 25–40.

Sadofsky, S. J., and G. E. Bebout (2004), Nitrogen geochemistry of subducting sediments: New results from the Izu-Bonin-Mariana margin and insights regarding global nitrogen subduction, *Geochem. Geophys. Geosyst.*, *5*, Q03I15, doi:10.1029/2003GC000543.

Stern, R. J., M. J. Fouch, and S. L. Klemperer (2003), An overview of the Izu-Bonin-Mariana subduction factory, in *Inside the Subduction Factory*, *Geophys. Monogr. Ser.*, vol. 138, edited by J. Eiler, pp. 175–222, AGU, Washington, D. C.

Straub, S. M., G. D. Layne, A. Schmidt, and C. H. Langmuir (2004), Volcanic glasses at the Izu arc volcanic front: New perspectives on fluid and sediment melt recycling in subduction zones, *Geochem. Geophys. Geosyst.*, *5*, Q01007, doi:10.1029/2002GC000408.

Tatsumi, Y. (2005), The subduction factory: How it operates in the evolving Earth, *GSA Today*, *15*, 4–10, doi:10:1130/1052-5173.

Taylor, R. N., and R. W. Nesbitt (1998), Isotopic characteristics of subduction fluids in an intra-oceanic setting, Izu-Bonin arc, Japan, *Earth Planet. Sci. Lett.*, *164*, 79–98.

Urbat, M., and T. Pletsch (2003), Pleistocene deep-sea sediment in ODP Hole 1149A, Nadezhda Basin: Sources, alteration, and age controls (0–800 ka) [online], *Proc. Ocean Drill. Program Sci. Results*, *185*, 21 pp. (Available at http://www-odp.tamu.edu/publications/185_SR)

Valentine, R. B., J. D. Morris, J. G. Ryan, K. A. Kelley, and S. H. Zheng (2002), $^{10}$Be systematics of incoming sediments and arc lavas at the Izu and Mariana convergent margin, *Eos Trans. AGU*, *83*(47), Fall Meet. Suppl., Abstract T71F-04.